Climate Dynamics (2025) 63:120
https://doi.org/10.1007/s00382-025-07622-x

ORIGINAL ARTICLE

Synergistic role of Atlantic SST and southern Russian steppe precipitation in subseasonal heat prediction over the Yangtze River Basin

Xin Qi[1] · Jianping Li[1,2] · Yang Zhao[1] · Zhaolu Hou[1] · Yazhou Zhang[1]

Received: 18 November 2024 / Accepted: 3 February 2025

Abstract
As a major environmental hazard, heat events can significantly impact human health, ecosystems, and social services. The accurate prediction of heat events at subseasonal timescales is essential for the mitigation of disasters. Based on observational data and reforecast data retrieved from the North American Multi-Model Ensemble (NMME) project, this study investigated the synergistic effect of the negative SST anomaly (SST^{-}) over the central North Atlantic and the positive precipitation anomaly ($PREC^{+}$) over the Southern Russian Steppe in June on the subseasonal heat prediction skill and the observed monthly maximum temperature (*Tmax*) in August over the Yangtze River Basin (YRB). The results first demonstrate that the NMME subseasonal heat prediction is unable to accurately reproduce the response to the forcing of two factors, indicating a lack of precision that NMME could be enhanced. The composite analysis of circulation further illustrates that the joint events can synergistically diminish the YRB *Tmax* in August through non-linear physical processes and then amplify the NMME subseasonal prediction bias. In particular, the inactive subseasonal wave activity over the mid-latitudes at the upper troposphere, the weakened Western North Pacific subtropical high, and the strengthened cyclonic anomalies at the lower troposphere are the principal processes responsible for the synergistic effect of SST^{-} and $PREC^{+}$. This study identifies the potential subseasonal precursors for the heat prediction over the YRB. It suggests that advancing subseasonal prediction should consider the synergistic effects of different land and sea signals in the preceding period.

Keywords Heat events · Subseasonal prediction · Yangtze River Basin · Synergistic effect

1 Introduction

Heat (referring to high temperature) has been recognized as a significant environmental and occupational health hazard that can have a substantial impact on public health, agriculture, and the socioeconomic system (e.g., Patz et al. 2005; Lu and Chen 2016; Perkins 2015). For instance, heat can impede the essential health services, diminish productivity in the workforce, and increases the risk of accidents. In recent years, the number of people exposed to extreme heat has increased exponentially as a consequence of global warming (Zhao et al. 2021). Heat-related mortality for people aged over 65 increased by roughly 85% between the 2000–2004 and 2017–2021 periods (Romanello et al. 2023). Hence, gaining an understanding of the causes and predictability of heat events is a crucial and challenging task, which will assist in enhancing risk mitigation strategies.

The Yangtze River Basin (YRB) is a hotspot for heat events in eastern China (Chen and Zhai 2017; Hsu et al. 2017; Hua et al. 2023). Previous studies have widely investigated the causes of heat events over the YRB at different time scales (Gao et al. 2018; Qi et al. 2019; Wang et al. 2023b; Zhang et al. 2023). In general, the most direct atmospheric circulation system associated with heat events

✉ Jianping Li
ljp@ouc.edu.cn

[1] Frontiers Science Center for Deep Ocean Multi-Spheres and Earth System (DOMES)/Key Laboratory of Physical Oceanography/Academy of Future Ocean, College of Oceanic and Atmospheric Sciences, Center for Ocean Carbon Neutrality, Ocean University of China, Qingdao 266100, China

[2] Laboratory for Ocean Dynamics and Climate, Qingdao Marine Science and Technology Center, Qingdao 266237, China

Published online: 13 February 2025

is an anomalous anticyclone accompanying subsidence in the lower troposphere, which is beneficial for increasing shortwave radiation and decreasing cloud cover (Luo and Lau 2017; Wang et al. 2017). At the interannual-to-decadal timescale, numerous studies have identified various factors from remote regions that affect the frequency and intensity of heat events, including the El Niño–Southern Oscillation (ENSO) (Zhou and Wu 2016), the summer monsoon (Liu et al. 2023; Wei et al. 2024; Zhu et al. 2012), the snow cover over the Tibetan Plateau (Wu et al. 2016), the sea surface temperature (SST) over the Indian Ocean (Hu et al. 2011), the Atlantic Multidecadal Oscillation (AMO) (Gao et al. 2019).

Based on the well-established causes of heat events, the heat prediction is also widely concerned (Diallo et al. 2024; Yang et al. 2024). Over the past few decades, seamless heat prediction from synoptical to decadal timescales has received ever-increasing attention with the development of high-performance computing and the optimization of parameterization schemes in numerical dynamic climate models (Vitart et al. 2017). The related research primarily focused on the evaluation of prediction skill (Qi and Yang 2019; Yang et al. 2018), the identification of predictability sources (Teng et al. 2013; Zhu and Li 2018), and the predictability limit (Quesada et al. 2012; Leach et al. 2021). For instance, Xie et al. (2020) report that three operational models participating in the Subseasonal to Seasonal Prediction (S2S) project have limited prediction skill over the YRB in terms of the proportion of correct predictions for summer heatwave days. Ma et al. (2023) explored the subseasonal predictability of a heat event over the YRB during the summer of 2012 and highlighted that the more accurate prediction of the Western Pacific subtropical high could improve the better temperature prediction.

Notably, subseasonal prediction occupies a relatively special position due to the fact that the prediction accuracy is contingent upon both the initial and boundary conditions (Mariotti et al. 2018). To date, there has been insufficient understanding of the subseasonal predictability sources for heat events, resulting in a restricted level of prediction skill (Tang et al. 2023a; Xie et al. 2020). In the intricate climate system of coupled land-air-sea, an investigation into the precursors that affect subseasonal heat prediction skill over the YRB may facilitate the enhancement of the physical parameterization scheme in the numerical model, thereby optimizing the prediction performance.

Note that Li et al. (2019a) proposed a novel approach to quantify the climatic synergistic effect of multiple factors, which has since been widely adopted in the scientific community (e.g.Sun and Li 2022; Tang et al. 2023b). For example, Wang et al. (2023a) found that the positive North Atlantic Oscillation (NAO) and the positive northwest Pacific SST anomaly in boreal summer act synergistically to influence the atmospheric circulation over central–eastern China, significantly increasing the local extreme heat events. Tang and Li (2024) identified a positive phase of the meridional tripole pattern of boreal autumn SST anomalies over the tropical and South Pacific has a synergistic effect with the winter negative NAO on the occurrence and amplitude of winter precipitation over southern Europe. In light of the synergistic notion, this methodology can be applied to the investigation of subseasonal heat prediction. Nevertheless, there is a paucity of comparable research.

Therefore, the purpose of this study is to address the following question: Are there any precursors that have a synergistic effect on subseasonal heat prediction over the YRB in summer, and, if such precursors exist, how do they affect it? The remainder of this article is organized as follows. Section 2 describes the data and methodology. Section 3 assesses the basic subseasonal *Tmax* prediction skill of the NMME and elucidates the identification of synergistic precursors. The physical mechanism underlying the synergistic effect is presented in Sect. 4. Finally, the discussion and conclusions are provided in Sect. 5.

2 Data and methods

2.1 Observations and reforecast data

The daily maximum temperature (*Tmax*) and atmospheric circulation fields (geopotential height, zonal winds and meridional winds on pressure levels) were sourced from the fifth-generation reanalysis dataset (ERA5) produced by the European Centre for Medium-Range Weather Forecasts (ECMWF) within the Copernicus Climate Change Service (C3S), which achieved at a high horizontal resolution of 0.25°×0.25° and 37 pressure levels in the vertical coordinate (Hersbach et al. 2020). The 1/4° daily Optimum Interpolation Sea Surface Temperature data (OISST v2.1) was provided by the National Oceanic and Atmospheric Administration (NOAA) (Huang et al. 2021). The precipitation data were derived from the Global Precipitation Climatology Project (GPCP) monthly dataset with the global coverage on a 2.5° grid (Schneider et al. 2013). For simplicity, the reanalysis, OISST and GPCP data are collectively referred to as observations. In this study, the period covered is June to August from 1982 to 2019, and monthly average variables are calculated by averaging the daily value.

The reforecast data generated from the North American Multi-Model Ensemble (NMME) project were used to assess the subseasonal performance of the dynamical model. The NMME is an experimental multi-model forecast system that contains a rich set of runs from many coupled

Table 1 A brief description of NMME models used in this study

Model Name	Members	Institute	Country
CanCM4i	10	Canadian Meteorological Centre	Canada
CanSIPS-IC3	10		
CanSIPSv2	20		
CMC1-CanCM3	10		
CMC2-CanCM4	10		
GEM-NEMO	10		
GFDL-CM2p1-aer04	10	Geophysical Fluid Dynamics Laboratory	United States of America
GFDL-CM2p5-FLOR-A06	12		
GFDL-CM2p5-FLOR-B01	12		
NASA-GEOSS2S	4	National Aeronautics and Space Administration	

models over a relatively long period from 1982 to the present and the hindcast data is available at the International Research Institute for Climate and Society (IRI) (Kirtman et al. 2014). The hindcasts of August with a horizontal resolution of 1.0°×1.0° were initiated from 1 July which yielded 1-month lead prediction. Given the full availability of the variables required for this study, 10 models were selected for analysis (Table 1).

2.2 Methods

2.2.1 Prediction assessment and statistical analysis

The ensemble mean of the selected NMME models is calculated to represent the results of subseasonal prediction. The observed and predicted anomalies at interannual timescales are obtained by removing their respective climatological means (defined over 1982–2019) and the linear long-term global warming trend. The mean square error (*MSE*), the root mean square error (*RMSE*) and the temporal correlation coefficient (*TCC*) are utilized to estimate the prediction skill of the NMME models. The first two statistics (*MSE* and *RMSE*) reflect the amplitude of the prediction bias, while the *TCC* indicates the similarity of the temporal evolution between the predicted and observed anomalies. The above common metrics are written as

$$MSE = \frac{1}{N}\sum_{i=1}^{N}(P_i' - O_i')^2,$$

$$RMSE = \sqrt{MSE},$$

$$TCC = \frac{1}{n}\sum_{i=1}^{n}\left(\frac{O_i'}{s_o}\right)\left(\frac{P_i'}{s_P}\right),$$

where O_i' (P_i') and s_o (s_P) denote the observed (predicted) anomalies and variances, N and n represent the total number of grid points and the length of the time series, respectively. As the raw *RMSE* takes only non-negative values, the standardized *RMSE* was calculated by subtracting the mean and dividing by the variance of the series. Following standardization, positive (negative) values thus represent relatively poor (good) prediction skill. In addition, the compositing technique (e.g., Gao et al. 2018; Yang et al. 2024) is conducted to investigate the common characteristic of anomalous atmospheric variables across different conditions, and the two-tailed *student's t-test* is applied to assess the statistical significance of the results.

Table 2 The definition of joint events and corresponding two types of single events

Type	Symbol	Notation
Joint events	$SST^{-} \oplus PREC^{+}$	Cases when SST^{-} and $PREC^{+}$ occur simultaneously
Single SST^{-} events	$SST^{-} \backslash PREC^{+}$	Cases when SST^{-} occurs without $PREC^{+}$
Single $PREC^{+}$ events	$PREC^{+} \backslash SST^{-}$	Cases when $PREC^{+}$ occurs without SST^{-}

2.2.2 Definition of synergistic effect

In order to ascertain the presence of synergistic factors on the subseasonal heat prediction over the YRV, this study employed the diagnostic tools of combined effect proposed by Li et al. (2019). As previously stated in the introduction, this study aimed to find the possible hotspots of anomalous SST over the North Atlantic and PREC in Eurasia. Here, each variable can be classified into positive, neutral and negative phases. For instance, if the positive PREC anomaly ($PREC^{+}$) and the negative SST anomaly (SST^{-}) are considered as a pair of synergistic drivers, three types of events can be defined accordingly (Table 2).

By comparing the different responses (R) to the three types of events, the kind of combined effect of the two factors (SST^{-} and $PREC^{+}$) can be determined. We defined the synergistic effect as follows:

$$|R|_{SST^{-} \oplus PREC^{+}} > max \left\{ |R|_{SST^{-} \backslash PREC^{+}}, |R|_{PREC^{+} \backslash SST^{-}} \right\}$$

2.2.3 Wave activity flux

Based on the quasi-geostrophic potential vorticity equation, the wave activity flux (WAF) was calculated to explore the propagation of subseasonal wave trains over the mid-latitudes. The two-dimensional WAF formulated by Takaya and Nakamura (2001) can be expressed as

$$W = \frac{1}{2|U|}\begin{bmatrix} \bar{u}\left(\psi'^{2}_{x} - \psi'\psi'_{xx}\right) + \bar{v}\left(\psi'_{x}\psi'_{y} - \psi'\psi'_{xy}\right) \\ \bar{u}\left(\psi'_{x}\psi'_{y} - \psi'\psi'_{xy}\right) + \bar{v}\left(\psi'^{2}_{y} - \psi'\psi'_{yy}\right) \end{bmatrix},$$

where W represents the horizontal WAF, U is the climatological mean wind speed, $\bar{u}$ and $\bar{v}$ are the climatology of zonal and meridional winds, respectively. ψ denotes the perturbation stream function and the subscript indicates partial derivative.

3 Identification of synergistic precursors affecting the subseasonal heat prediction over the Yangtze River Basin

To understand the general subseasonal heat prediction skill of NMME models over the YRB in August, we first examined the climatological prediction of *Tmax* at a one-month lead. In comparison to the observed average monthly *Tmax* of 29.7 °C over the target region, the one-month-ahead hindcast of 30.3 °C yielded comparable results (Fig. 1a&b). However, the prediction of the heat center (high-temperature region) exhibits a notable northward shift, suggesting that the spatial distribution of the heat predicted by NMME at the subseasonal timescale remains insufficient. The potential sources of predictive uncertainty are diverse. For instance, the technical limitations of physical parameterization schemes and grid resolution in the numerical models

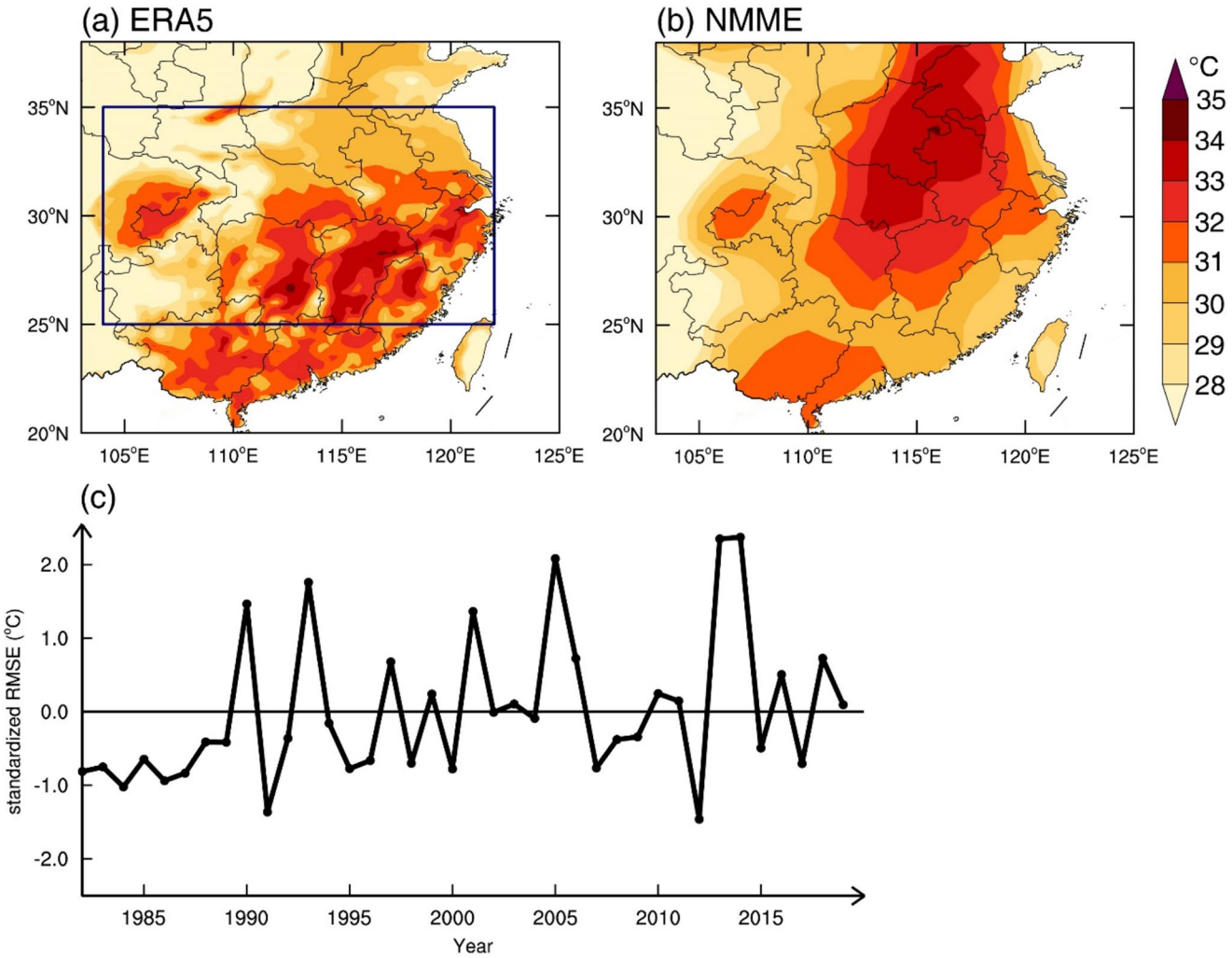

Fig. 1 **a** Observed climatological mean August maximum temperature (*Tmax*) in the ERA5 data (shaded; units: °C). The base period for the climatological mean is 1982–2019. The box denotes the location of the Yangtze River Basin (YRB, 25°–35°N, 104°–122°E). **b** Same as **a** but for the subseasonal predicted results with one-month lead time using the NMME reforecast data. **c** Standardized *RMSE* time series obtained from the observed and predicted *Tmax* over the YRV region

preclude them from accurately reproducing realistic coupling processes (e.g., Becker et al. 2014; Xu et al. 2021). Additionally, the accuracy of initial and boundary conditions has been reported to have an effect on subseasonal prediction results (e.g., Qi and Yang 2019; Yang et al. 2018, 2024).

With respect to the its prediction performance by year, the fair sign consistency ratio (~61%) and the relatively low correlation coefficient (0.21) between the observed and predicted *Tmax* averaged across the YRB region indicate that the prediction skills require further improvement. Moreover, the standardized *RMSE* time series depicted in Fig. 1c illustrates the significant interannual variation in the NMME's subseasonal heat prediction skills, reflecting the inherently unstable predictive performance. Therefore, it would be beneficial to investigate the possible factors that influence heat prediction skills at the subseasonal timescale. In this study, the *RMSE* is employed as a measure of subseasonal heat prediction skills, which provides the basis for the subsequent identification of the synergistic precursors.

Since anomalous SST over the ocean and precipitation over the land are frequently used predictors in operational climate forecasts, we calculated the temporal correlation coefficient between the *RMSE* of the predicted August *Tmax* over the YRB at 1-month ahead and the observed SST anomaly, as well as the land precipitation anomaly, in June. As shown in Fig. 2, the predicted *RMSE* of the *Tmax* over the YRB and the anomalous predictors over the different regions present a diverse correlation relationship. Two regions with high correlation values can be clearly identified: the central North Atlantic (25°–34°N, 39°–54°W) and the Southern Russian Steppe (48°–54°N, 30°–56°E). It is found that the SST (precipitation) anomaly over the central North Atlantic (the Southern Russian Steppe) in June exhibits a significant negative (positive) correlation with the predicted *RMSE* of *Tmax* over the YRB. This indicates that the cooling SST (SST^-) over the central North Atlantic and the rainy conditions ($PREC^+$) over the Southern Russian Steppe may amplify the NMME prediction bias of *Tmax*, resulting in a worse subseasonal prediction skill because of the higher *RMSE* values corresponding to the lower prediction skill. Here, it was imperative to underscore the lead-lag relationship that the observed forcing in June was already known when the predicted *Tmax* initiated at 1 July by NMME.

Can the SST^- in the central North Atlantic and the $PREC^+$ in the Southern Russian Steppe synergistically affect subseasonal heat prediction skills over the YRB? To answer this question, we calculated the regional average anomalies of the two factors for each June and examined the response of the subseasonal prediction skills produced by the NMME (Fig. 3). As illustrated in Fig. 3a, the correlation coefficient between the anomalous SST and precipitation over the respective area is nearly zero (r=-0.03), thereby indicating that they are statistically independent factors of each other and the results facilitate comprehension of the synergistic effect. Figure 3b further presents the corresponding *RMSE* of the predicted August *Tmax* over the YRB at a one-month lead time. Considering the different configurations of anomalous conditions observed in the two precursors, we identified three years (1990, 1993, and 2005) for which the pairs of SST^- and $PREC^+$ occurred within the top five *RMSE* values. Naturally, the observational SST^- over the central North Atlantic and $PREC^+$ over the Southern Russian Steppe in June are regarded as a pair of synergistic drivers in this study. Based on it, the occurrence years of joint events ($SST^- \oplus PREC^+$, red dots in Fig. 3b), single SST^- events ($SST^- \setminus PREC^+$, blue dots), and single $PREC^+$ events ($PREC^+ \setminus SST^-$, green dots) are determined. The composite average response of the *RMSE* for the three types of events is given in Fig. 3c. It is noticeable that the *RMSE* for the joint $SST^- \oplus PREC^+$ events is much larger than for the other two single events, which means that the NMME subseasonal heat prediction has a worse performance over the YRB when the SST^- over the central North Atlantic and the $PREC^+$ over the Southern Russian Steppe occur synchronously in early summer. Hence, the results preliminarily

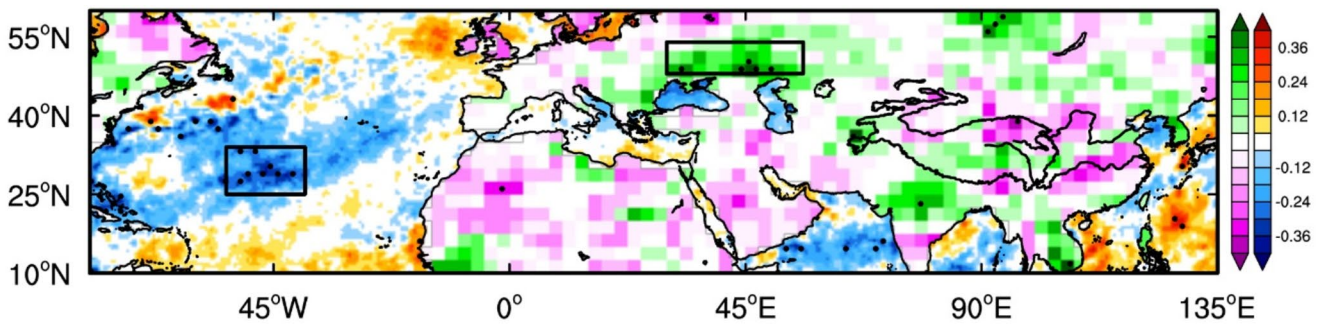

Fig. 2 Correlation map between the *RMSE* of the NMME predicted *Tmax* over the Yangtze River Basin in August and the sea surface temperature (ocean)/precipitation (land) anomaly in June. Dots indicate the significant results at the 95% confidence level based on the Student *t*-test. The boxes represent the location of the central North Atlantic (25°–34°N, 39°–54°W) and the southern Russian steppe (48°–54°N, 30°–56°E), respectively

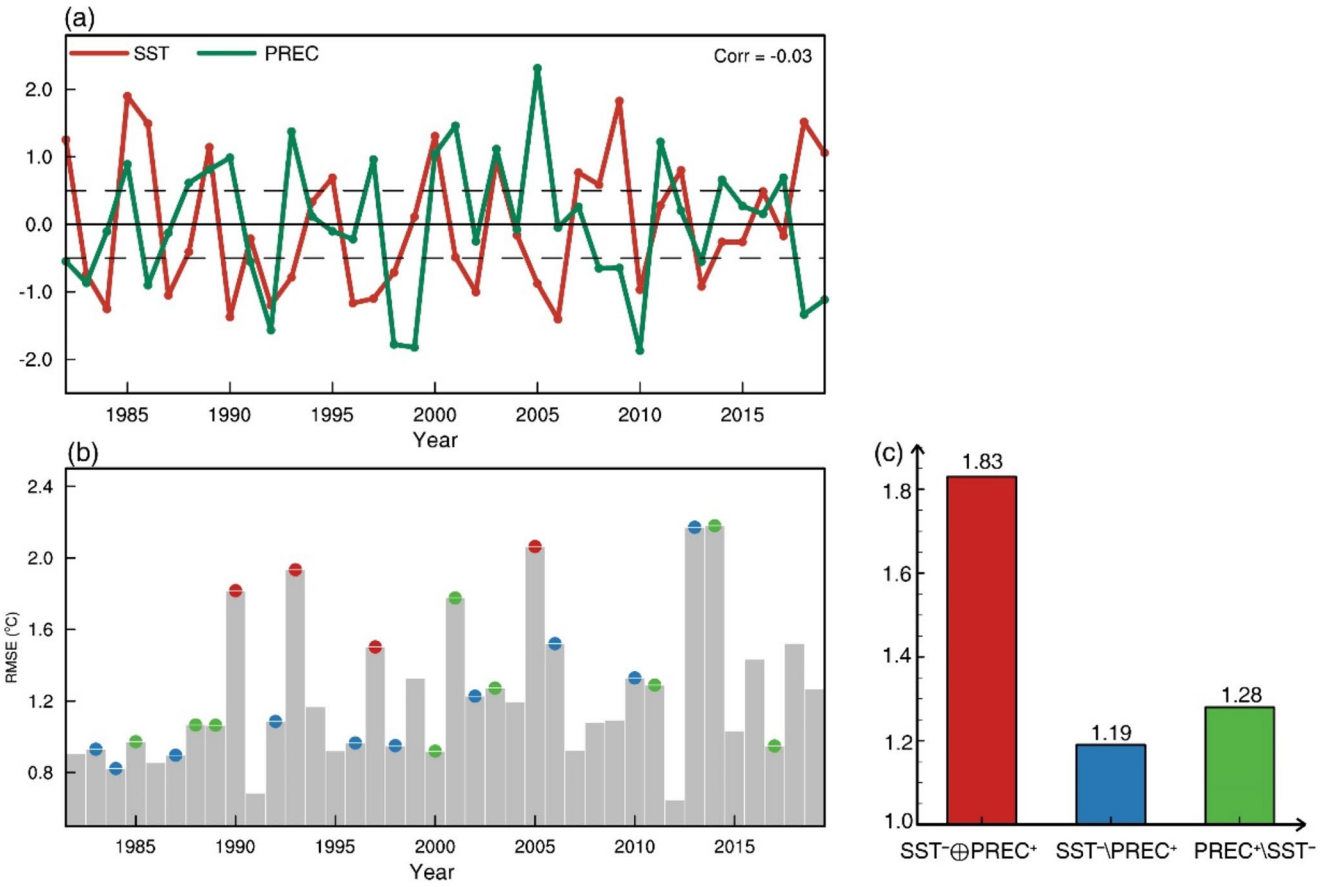

Fig. 3 **a** Standardized time series of area-averaged anomalous SST over the central North Atlantic (red line) and precipitation over the southern Russian steppe (green line) in June. Dashed black lines represent ± 0.5 standard deviation. **b** Raw *RMSE* time series obtained from the observed and predicted *Tmax* over the Yangtze River Basin region in August. The red, blue and green dots represent the occurrence of joint events, single SST^- events, and single $PREC^+$ events, respectively. **c** The mean *RMSE* for the three types of events above

indicate that there may be a synergistic effect between the SST^- over the central North Atlantic and $PREC^+$ over the Southern Russian Steppe.

Notice that the calculation of *RMSE* involved the difference between the prediction and observation, we next conducted a comprehensive budget analysis based on the MSE to ascertain whether the observed and predicted results still exhibited divergence across different types of events (Fig. 4). The MSE can be decomposed into three summation terms: observation $\left(\frac{1}{n}\sum_{i=1}^{n} {O'_i}^2\right)$, prediction $\left(\frac{1}{n}\sum_{i=1}^{n} {P'_i}^2\right)$, and the product of observation and prediction $\left(-\frac{1}{n}\sum_{i=1}^{n} 2O'_i P'_i\right)$. Here, the calculations were performed using the anomalous values, the first two terms can be regarded as reflecting the observed and predicted absolute intensity, respectively. The third term captures the overall sign consistency of the *Tmax* anomalies between the observation and prediction. In general, an increase in consistency will result in a decrease in MSE value. The results demonstrate that the observed summation term (purple bars) produces comparable contributions to the MSE, whose composite response to the joint $SST^-\oplus PREC^+$ events is greater than that either to the $SST^- \setminus PREC^+$ or $PREC^+ \setminus SST^-$ single events. However, according to the predicted summation term (green bars), the response to the joint events is only slightly higher than that to the other single events, which is not statistically significant. This result reveals that the subseasonal heat prediction skill of the NMME is unable to accurately replicate the actual response to the forcing of SST^- over the central North Atlantic and the $PREC^+$ over the Southern Russian Steppe. Furthermore, the summation term of the product of observation and prediction (blue bars) displays an absence of evident response differences and a relatively small proportion in the MSE to the three types of events. Therefore, it implies that the SST^- over the central North Atlantic and the $PREC^+$ over the Southern Russian Steppe in June can exert a synergistic effect not only on the subseasonal heat prediction skill, but also on the August *Tmax* over the YRB.

Figure 5 provides further evidence of the aforementioned synergies in terms of the correlation relationship. We first compared correlation coefficients between the precipitation

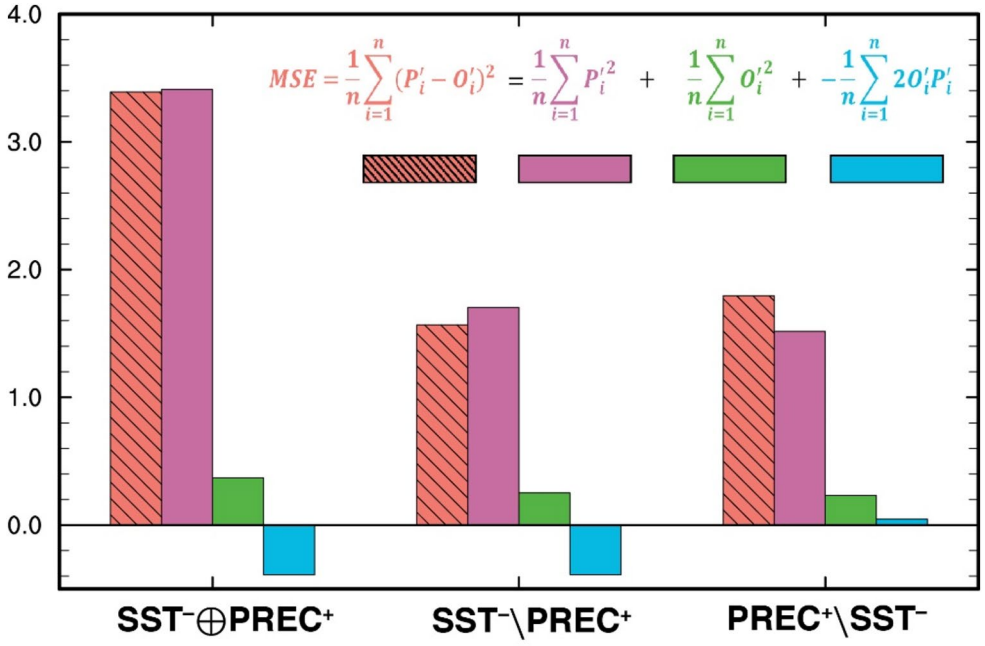

Fig. 4 The Mean square error (MSE) of *Tmax* budget terms averaged over the Yangtze River Basin for joint events, single $SSTA^-$ events, and single $Prep^+$ events, respectively. From left to right: MSE (red shadow), the observation term (purple), the prediction term (green), and the interaction term of observation and prediction (blue)

anomaly over the southern Russian steppe in June and the *RMSE* of *Tmax* over the YRB in August for all years, years with warming SST and years with cooling SST over the central North Atlantic, respectively (Fig. 5a). In general, the *RMSE* is positively correlated with anomalous precipitation ($r=0.33$), suggesting that the increased rainfall over the southern Russian steppe may amplify the predicted *RMSE* and reduce the subseasonal prediction skill. Nevertheless, the correlations demonstrate the opposite changes under different anomalous SST conditions over the central North Atlantic. Specifically, the correlation between the precipitation anomaly and the *RMSE* of *Tmax* shows non-significant negative relationship ($r=-0.23$) in the warm SST years, while it exhibits a more significant positive relationship ($r=0.53$) in the cold SST years than in the whole years. This result reflects the combined effect of the SST^- and $PREC^+$, illustrating a synergistic outcome. Similarly, Fig. 5b displays correlation coefficients between the SST anomaly over the central North Atlantic in June and the *RMSE* of *Tmax* over the YRB in August for all years, as well as for rainy years and dry years over the southern Russian steppe, respectively. The *RMSE* presents a negative correlation relationship with SST anomaly ($r=-0.33$) across all years, thus indicating that the negative SST anomalies over the central North Atlantic are conducive to increasing the predicted bias. Especially in the wet years, the correlation between the *RMSE* and the anomalous SST is more notable ($r=-0.67$), compared to that in the dry years ($r=-0.1$). It can be therefore confirmed that the $SST^-\oplus PREC^+$ plays a synergistic role in subseasonal heat prediction over the YRB.

In addition to the *RMSE*, the synergistic relationship between the $SST^-\oplus PREC^+$ events and the observed August *Tmax* over YRB can also be detected (Fig. 5c, d). It is evident that the anomalous precipitation over the southern Russian steppe has a more pronounced negative correlation with the *Tmax* in the cold SST years ($r=-0.43$) than in the whole years ($r=-0.32$) and in the warm SST years ($r=-0.10$) (Fig. 5c). This finding suggests that the positive precipitation anomaly over the southern Russian steppe is more conducive to reducing the YRB *Tmax* and weakening heat intensity when the SST over the central North Atlantic exhibits a negative anomaly. With regard to the correlation between the *Tmax* and the SST anomaly, the correlation coefficient is still largest ($r=0.16$) in the rainy years over the southern Russian steppe, although the correlation coefficients are relatively weak under the three conditions (Fig. 5d). In brief, the SST^- over the central North Atlantic and the $PREC^+$ over the Southern Russian Steppe in June are identified as two synergistic precursors that can influence the August *Tmax* and subseasonal heat prediction skill over the YRB.

4 Possible physical mechanism underlying the synergistic effect of Atlantic SST and southern Russian steppe precipitation

Since the subseasonal heat prediction skill carried out by the NMME is constrained in its scope to respond to the forcing of the joint events $SST^-\oplus PREC^+$ (Fig. 4), this section will primarily address its synergistic effect on the observed *Tmax* over the YRB. Locally speaking, the composite patterns of the anomalous *Tmax* and the horizontal winds at 850 hPa over the South China for different events are first presented

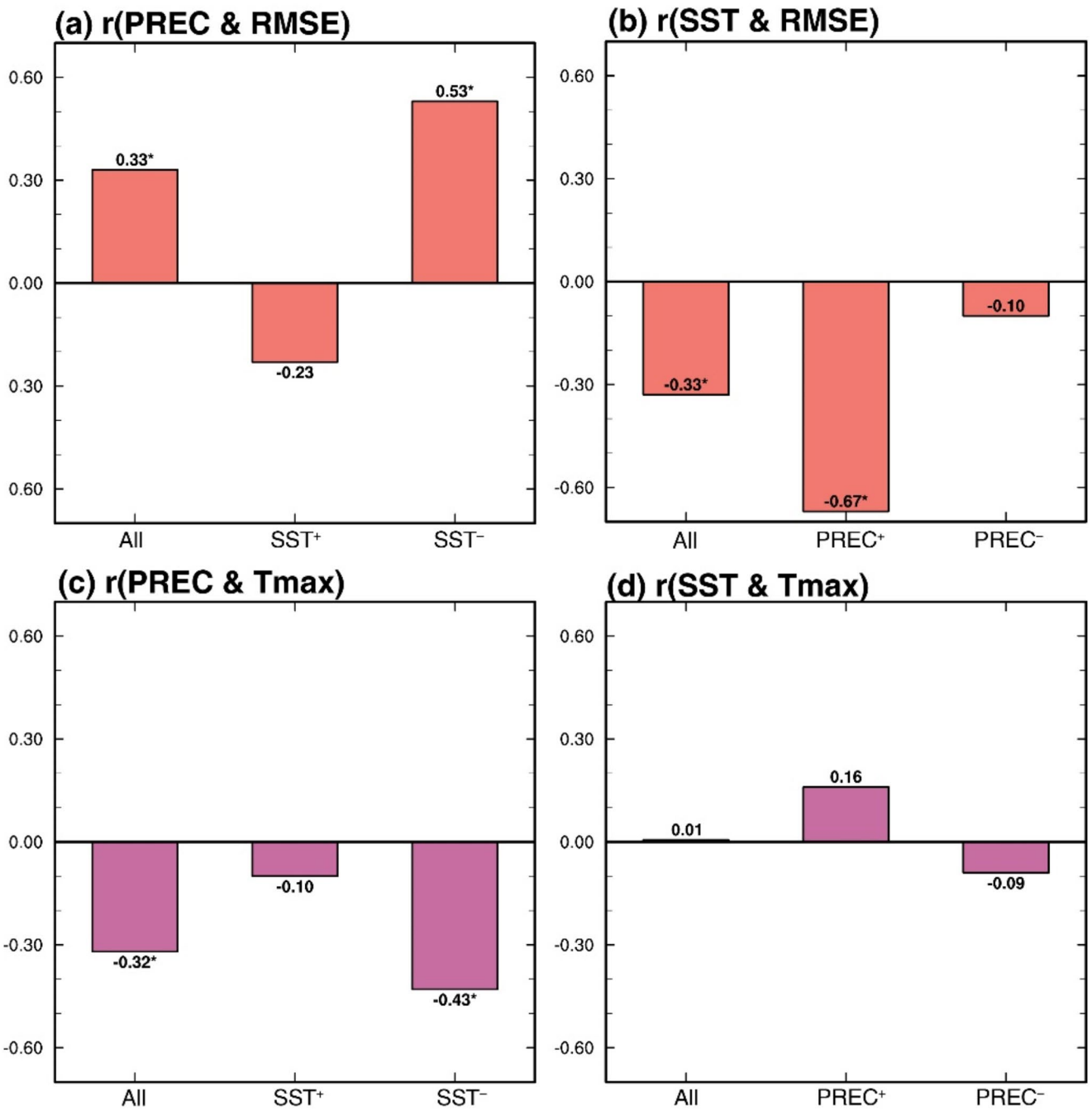

Fig. 5 **a** Correlation coefficients between the precipitation anomaly averaged over the southern Russian steppe in June and the *RMSE* of *Tmax* averaged over the Yangtze River Basin in August for all years, years with positive SST anomaly and years with negative SST anomaly, respectively. **b** Correlation coefficients between the SST anomaly averaged over the central North Atlantic in June and the *RMSE* of *Tmax* averaged over the Yangtze River Basin in August for all years, years with positive precipitation anomaly and years with negative precipitation anomaly, respectively. **c** and **d** are the same as **a** and **b** except for *Tmax*

in Fig. 6a–c. When the SST^- over the central North Atlantic and the $PREC^+$ over the Southern Russian Steppe emerge synchronously in June (i.e., joint events $SST^- \oplus PREC^+$), a significant negative anomalous *Tmax* center appears over the eastern part of the YRB in August, accompanied by the apparent cyclonic circulation anomaly (Fig. 6a). However, for the single SST^- events ($SST^- \backslash PREC^+$), a warm anomaly is observed in the northeastern part of the YRB, which is associated with clear anticyclonic anomalies (Fig. 6b). In contrast, the response of the single $PREC^+$ events ($PREC^+ \backslash SST^-$) is characterized by a weaker cold anomaly, modulated by the wind shear of an easterly (westerly) wind anomaly in

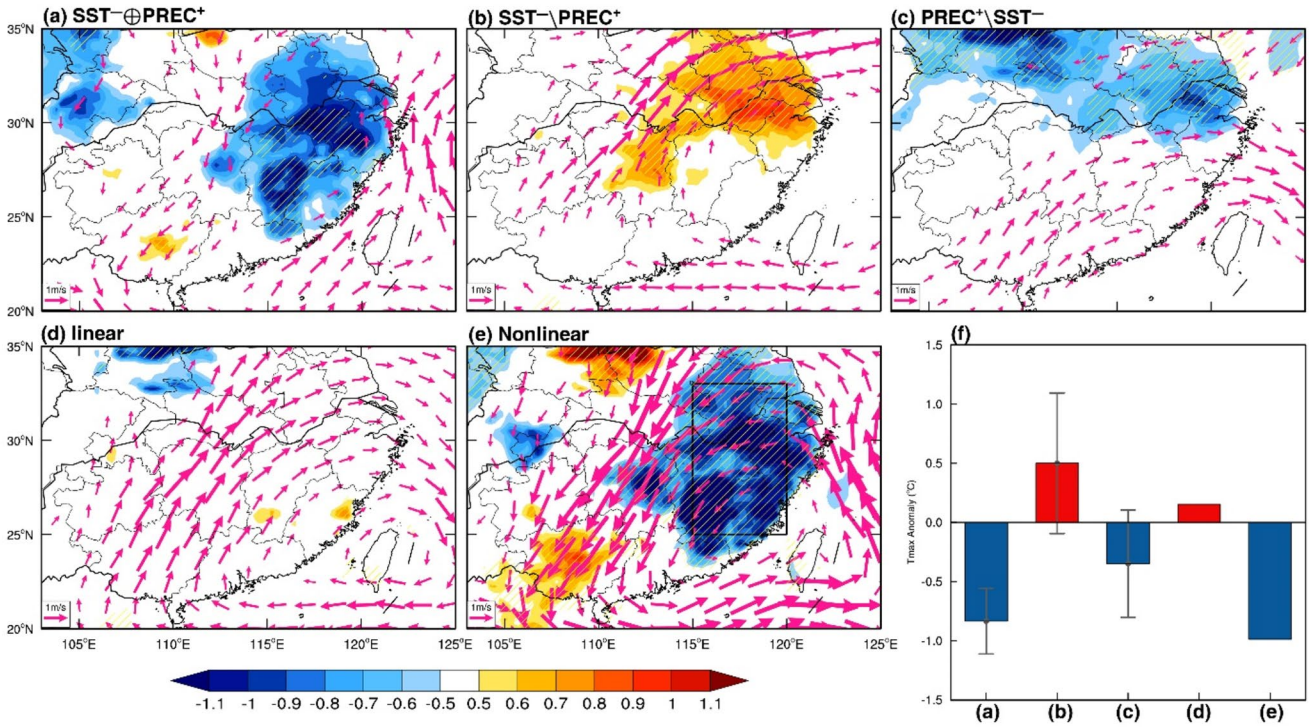

Fig. 6 Composite anomalies of *Tmax* (shaded; units: °C) and winds at 850 hPa (vectors; units: $m \cdot s^{-1}$) in August for **a** joint events, **b** single $SSTA^-$ events, **c** single $Prep^+$ events, **d** linear superposition of **a** & **b**, and **e** difference between **a** & **d**, respectively. Slash shadows indicate the significant areas with a 90% confidence level. **f** Area-averaged *Tmax* anomaly over the target region (black box, 25°–33°N, 115°–120°E) in **a**–**e**. The line variation over the bars indicates the standard deviation

the northern (southern) side (Fig. 6c). The results revealed that there were disparate anomalous *Tmax* responses for the three types of events, and the joint events $SST^-\oplus PREC^+$ displayed the most pronounced response compared to the other two single events.

Due to the independent relationship of the anomalous SST over the central North Atlantic and precipitation over the Southern Russian Steppe (Fig. 3a), we further explored the linear superposition and nonlinear effect of the two factors on the target region (Fig. 6d–f). In this context, the linear effect is defined as the superposition of the response of the single SST^- events and $PREC^+$ events, and the nonlinear effect is calculated as the difference between the joint events response and the linear superposition response of the two single events. As demonstrated in Fig. 6d, the aggregate of the circulation responses manifests an anticyclonic anomaly that is analogous to that of $SST^-\backslash PREC^+$, whereas the linear superposition result of the *Tmax* responses evinces no discernible signal since the isolated responses to single SST^- events and single $PREC^+$ events are offset against each other. Conversely, the nonlinear effect of the $SST^-\oplus PREC^+$ illustrated in Fig. 6e portray a significant cold anomaly and anomalous cyclonic circulation at the lower troposphere level over the eastern China, which is quite similar to the observed response to the joint events (Fig. 6a). Furthermore, the nonlinear effect of SST^- and $PREC^+$ on the August anomalous *Tmax* is of particular importance (Fig. 6f), implying that the relationship between the joint $SST^-\oplus PREC^+$ events and the anomalous response is governed by intricate dynamic processes. That is, the composite results for different events demonstrate that the above synergistic effect may enhance the nonlinear response of *Tmax* over the YRB.

In the following, the observed circulation anomalies at upper and middle troposphere under different events were examined to investigate the potential linkage between the identified forcing factors and the subsequent *Tmax* response over the YRB. Figure 7 shows the composite anomalies of geopotential height and horizontal winds at 200 hPa in August. When SST^- and $PREC^+$ occur synchronously in June, the most predominant feature over the mid-latitude region in August is a broad low-pressure belt that extends from the North Atlantic to the Kamchatka Peninsula in the Russian Far East (Fig. 7a). The cyclonic anomaly centers can be identified both over the central North Atlantic and the Southern Russian Steppe, which indicates that the anomalous negative geopotential height caused by the cold SST and the more-than-normal precipitation over the respective region in June can persist to the late summer. In comparison, the observed circulation patterns to the single events of $SST^-\backslash PREC^+$ and $PREC+\backslash SST^-$ are significantly

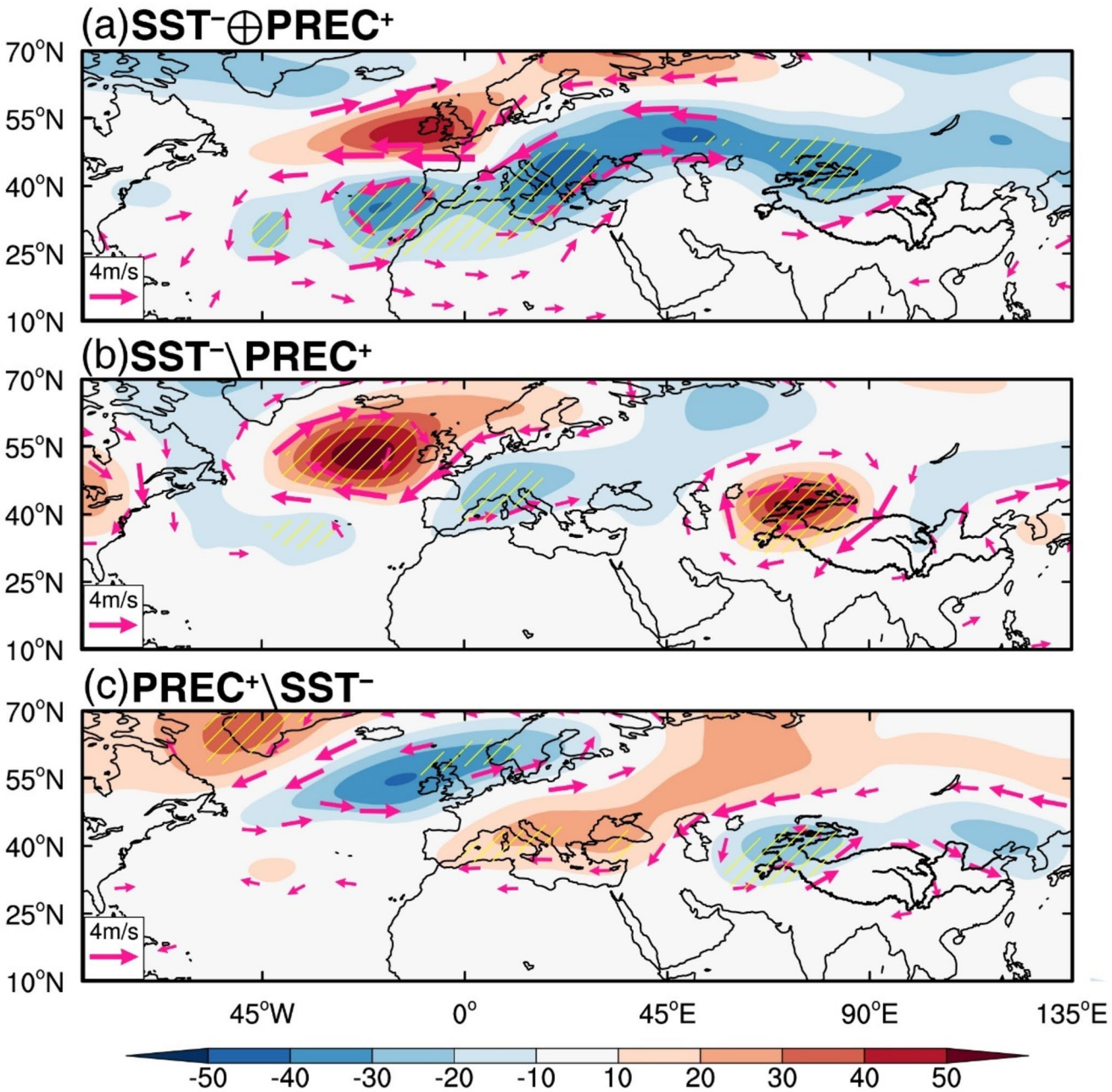

Fig. 7 Composite anomalies of geopotential height (shaded; units: gpm) and winds (vectors; units: $m \cdot s^{-1}$) at 200 hPa in August for **a** joint events, **b** single $SSTA^{-}$ events, and **c** single $Prep^{+}$ events, respectively. Slash shadows indicate the significant areas with a 90% confidence level

distinct from that associated with the joint events, resulting in a different *Tmax* response. For the $SST^{-}\backslash PREC^{+}$ events, the anomalous negative center of geopotential height over the central North Atlantic remains while a significant anticyclonic anomaly develops over the northwestern Tibetan Plateau (Fig. 7b). For the $PREC^{+}\backslash SST^{-}$ events, the response is in anti-phase with that of $SST^{-}\backslash PREC^{+}$ events, accompanied by the anomalous cyclones over the northern North Atlantic and the northwestern Tibetan Plateau, respectively (Fig. 7c). The presented findings indicate that the synergistic factors can exert a distinctive circulation response through a non-linear process.

Previous studies have reported that the intraseasonal wave train over the mid-latitude region has a considerable influence on the occurrence of YRB heat events (e.g., Gao et al. 2018). Additionally, extratropical Rossby wave can contribute to the formation of a deep high-pressure system over the YRB (Qi et al. 2019). To further analyze the synergistic effect of SST^{-} and $PREC^{+}$ on the wave energy propagation, Fig. 8 depicts the difference between the wave activity

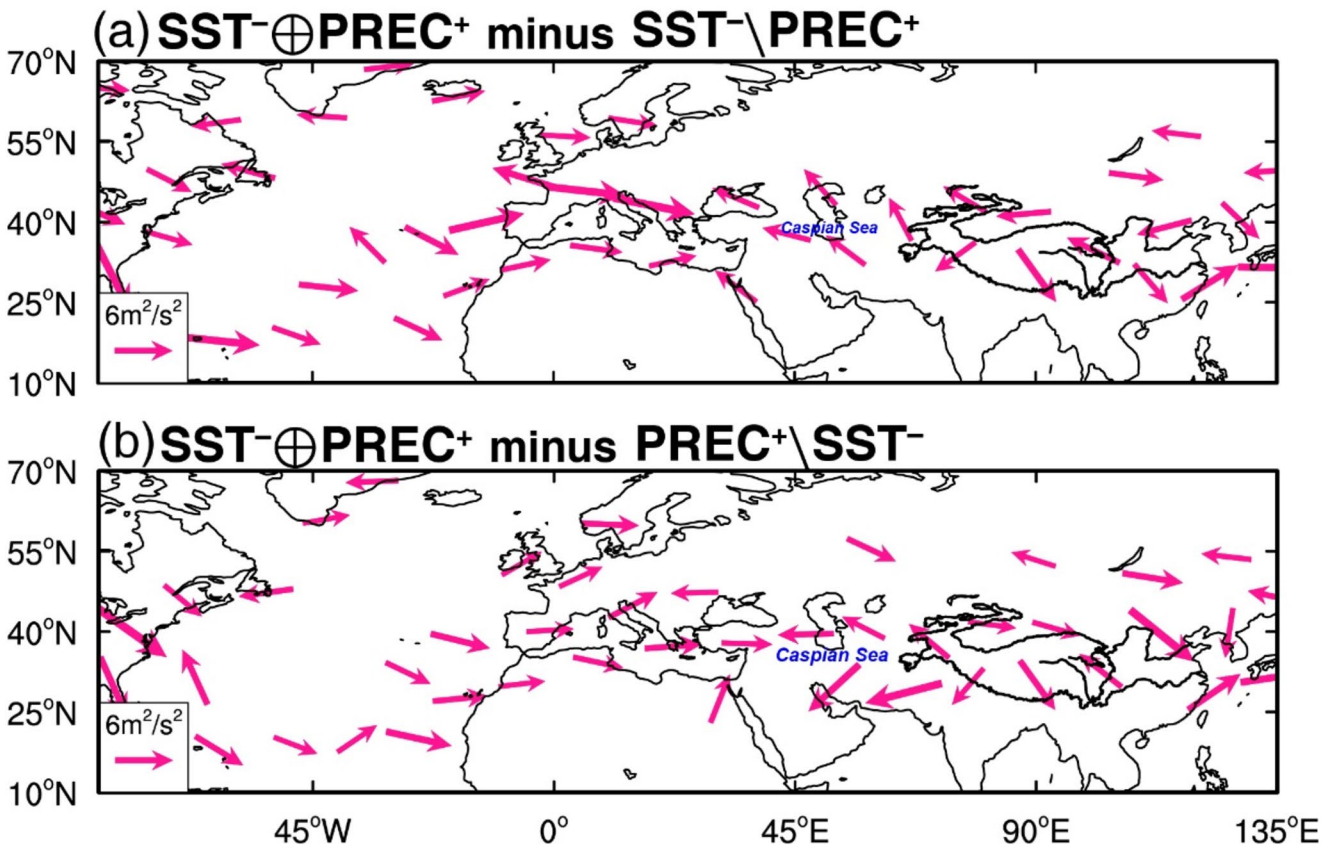

Fig. 8 Composite difference of wave activity flux (vectors; units: $m^2 \cdot s^{-2}$) at 200 hPa in August between joint events and **a** single $SSTA^-$ events (**b** single $Prep^+$ events)

flux of the joint events and that of the two single events. A striking difference is observed in the mid-latitudes along the westerly jet, which is in accordance with the position of the low-pressure belt in the $SST^-\oplus PREC^+$ events. It is noted that an anomalous easterly zonal component of the wave activity flux is detected across the extended Caspian Sea region, indicating that the propagation of the wave train is impeded when joint events occur. Namely, the Rossby wave are less active at the upper troposphere in the joint $SST^-\oplus PREC^+$ events than in any single event, which may subsequently reduce the heat intensity over the downstream area.

At the middle troposphere, the Western North Pacific subtropical high (WNPSH) is strongly associated with heat events over the YRB. Finally, the local response of the area-averaged geopotential height anomaly at 500 hPa over the target region was compared under three kinds of events (Fig. 9). According to the result shown in Fig. 9a, there is a negative response in the joint $SST^-\oplus PREC^+$ events (red bar) and the single $PREC^+$ events (green bar), whereas a positive response is observed during the single SST^- events (blue bar). Physically, the positive (negative) anomaly of the 500 hPa geopotential height is favorable for the enhancement (attenuation) of the WNPSH, which then leads to an increase (decrease) in surface temperature. As such, the SST^- single events can cause warming over the YRB, while the synergistic effect of SST^- and $PREC^+$ produces a more notable cooling than that of $PREC^+$ single events. This outcome aligns with the observed *Tmax* response presented in Fig. 6f. Moreover, the autocorrelation analysis of the geopotential height series reveals that the joint $SST^-\oplus PREC^+$ events exhibits the fastest decline response compared to the other single events. It can be inferred that the synergistic effect potentially results in a less stability of the WNPSH, thereby having an adverse impact on the local warming over the YRB (Fig. 9b).

5 Discussion and conclusions

5.1 Discussion

The observational analysis identified that the SST^- over the central North Atlantic and the $PREC^+$ over the Southern Russian Steppe in June can synergistically influence the August *Tmax* and subseasonal heat prediction skill over

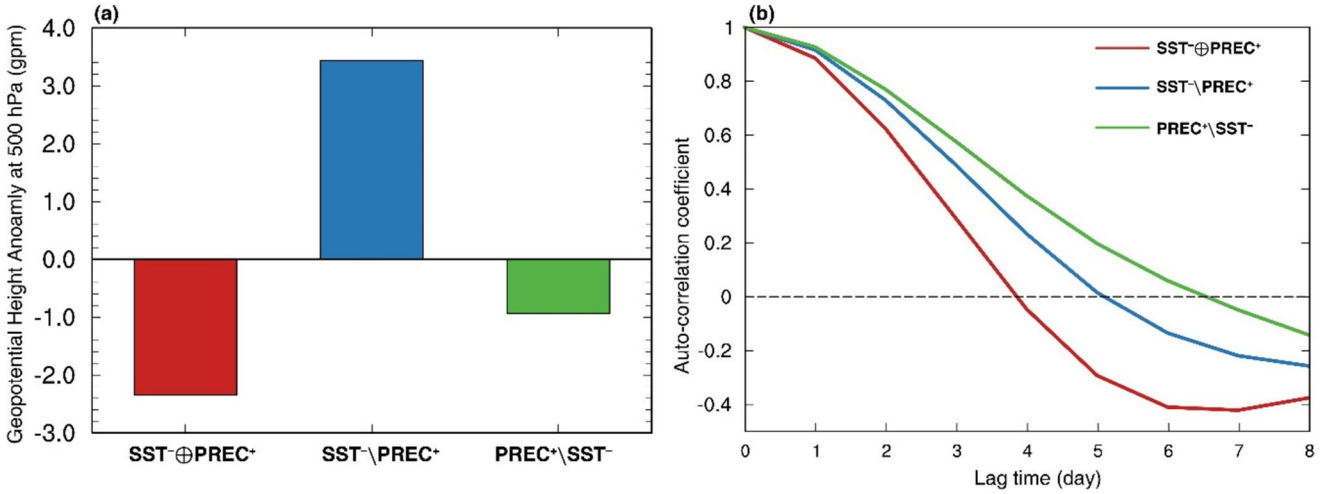

Fig. 9 **a** Area-averaged values (units: gpm) and **b** Auto-correlation coefficient at different lag days of the geopotential height anomaly at 500 hPa over the target region (25°–33°N, 115°–120°E) in August for joint events, single $SSTA^-$ events, and single $Prep^+$ events, respectively

the YRB. In light of the unsatisfactory prediction performance produced by the NMME, we attempted to construct a novel prediction model using multiple linear regression techniques to optimize the accuracy of the *Tmax* prediction. The traditional statistical model can be expressed as:

$$Tmax_{Ano} = 0.1 \times SST_{Ano} - 0.6 \times PREC_{Ano} + SST_{Ano} \times PREC_{Ano} \quad ,$$

where $Tmax_{Ano}$ denotes the predicted August *Tmax* anomaly averaged over the key region of the YRB (see Fig. 6e), SST_{Ano} and $PREC_{Ano}$ denote the observed SST anomaly over the central North Atlantic and precipitation anomaly over the Southern Russian Steppe in June, respectively.

Figure 10a portrays the regional average anomalies over the target area derived from the observational data (red line), NMME reforecast data at a one-month lead (orange line), and the above statistical prediction model (orange line). A comparison of the sign consistency ratio indicates an enhancement in the outcomes predicted by the statistical prediction model, with a rise from 55.26 to 63.16% compared to the NMME prediction (Fig. 10b). With regard to the correlation relationship, there is a notable improvement in the value from −0.04 to 0.43 (Fig. 10c). This finding suggest that the empirical prediction model may offer superior performance compared to the NMME dynamical model. Furthermore, the two identified synergistic precursors have the potential to be applied in the subseasonal heat prediction.

To be sure, it is imperative to recognize that the proposed non-linear synergistic effect of $SST^-\oplus PREC^+$ is based on the observational diagnostic. The intricate cross-month bridge may be attributed to the memory of anomalous soil moisture, which modulates the pathways and intensity of atmospheric Rossby waves (Wang et al. 2023a). It requires validation through numerical experiments in the next work. Given the inherent complexity of the climate system, the methodology deployed in this study to identify synergistic factors affecting sub-seasonal prediction skills warrants further investigation and application.

5.2 Conclusions

The accurate prediction of subseasonal heat events is of vital importance for the mitigation of disasters. Based on the evaluation of the NMME subseasonal perdition skill, this study investigated the proceeding factors influencing the subseasonal heat prediction skill over the YRB from the perspective of synergistic effect. Based on the evaluation of the NMME prediction performance at the subseasonal timescale, this study has investigated the factors that influence the subseasonal heat prediction skill over the YRB from the perspective of the synergistic effect. The results indicate that there is still much room for enhancement in the NMME subseasonal prediction skill of monthly mean *Tmax* over the YRB. More importantly, the synergistic analysis identified a pair of precursors—the negative SST anomaly over the central North Atlantic and the positive precipitation anomaly over the Southern Russian Steppe in June—that can influence the subseasonal heat prediction skill as well as the observed August *Tmax* over the YRB. The composite circulation results shows the joint $SST^-\oplus PREC^+$ events can synergistically weaken the heat intensity over the YRB in August through non-linear physical processes and amplify the NMME subseasonal prediction bias. Figure 11 summarized the potential physical mechanism of this synergistic effect. When the SST^- and $PREC^+$ occur simultaneously in June, the observed decrease in August *Tmax* over the YRB

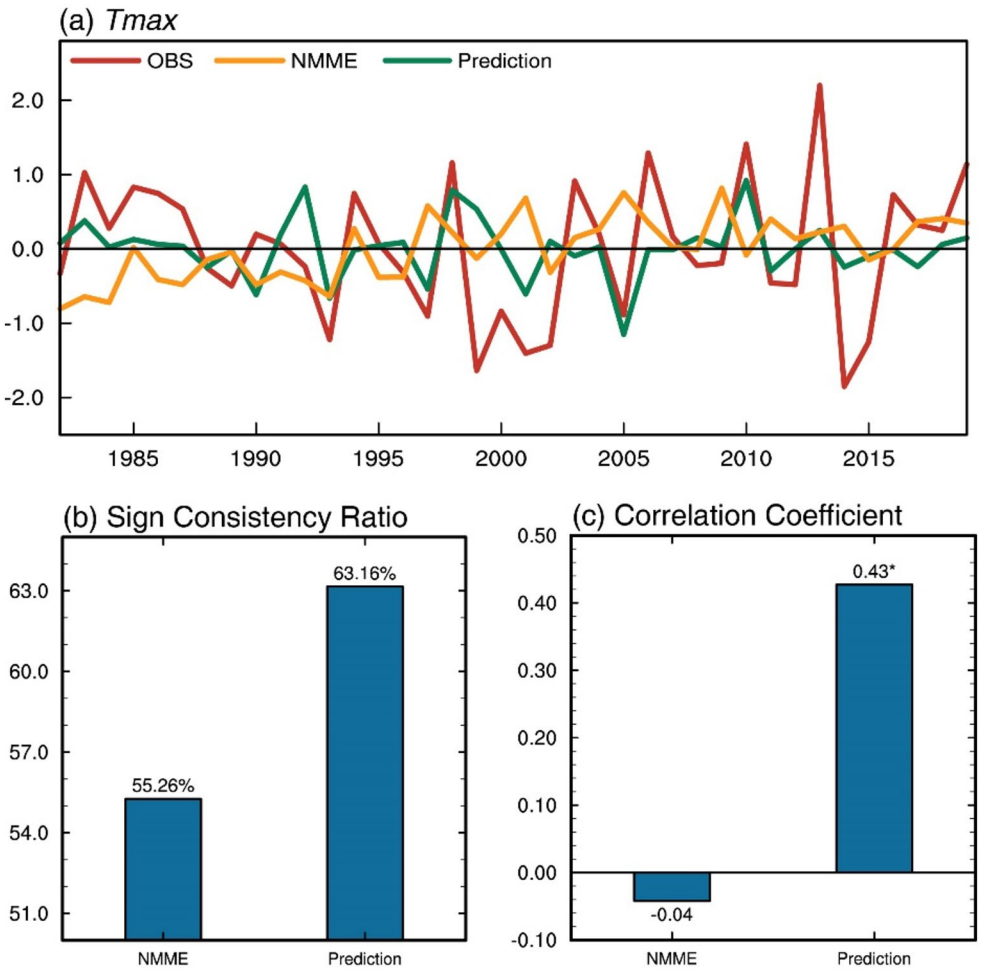

Fig. 10 **a** Time series of the area-averaged *Tmax* anomaly in August over the target region (25°–33°N, 115°–120°E) obtained from the ERA5 data (red line), the NMME reforecast data (orange line), and the empirical prediction model (green line). **b** Sign consistency ratio and **c** Correlation coefficients of the *Tmax* anomaly in August over the target region between the results of the ERA5 data and the NMME reforecast data / the empirical prediction model (blue bars)

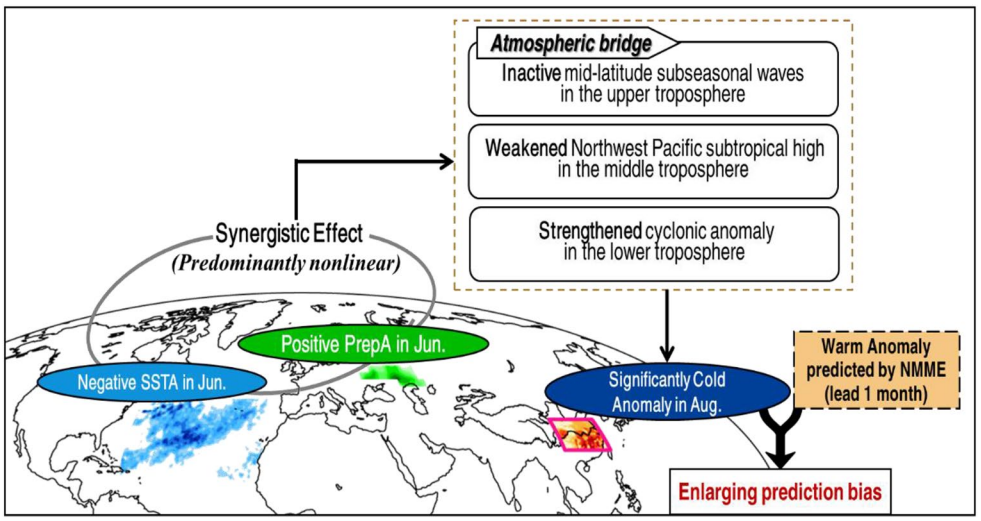

Fig. 11 The schematic diagram illustrating the synergistic effect of the cold Atlantic SST and rainy conditions over the southern Russian steppe on the amplification of the subseasonal heat prediction bias over the Yangtze River Basin

can be primarily attributed to three nonlinear responses: the inactive subseasonal wave activity over the mid-latitudes in the upper troposphere, and the weakened WNPSH, and the strengthened anomalous cyclone at the lower level. The current study provides empirical precursory signals for the subseasonal heat prediction, highlighting that advancing subseasonal prediction should take into account the synergistic effects of diverse land and sea signals in the preceding period.

Acknowledgements We would like to acknowledge the help of NCEP, IRI, and NCAR personnel in creating, updating, and maintaining the NMME archive.

Author contributions Xin Qi and Jianping Li designed the study and contributed to the data analysis, figures, and writing of the paper. All authors commented on previous versions of the manuscript. All authors read and approved the final manuscript.

Funding Jianping Li is supported by the National Natural Science Foundation of China Project (42288101 and 42130607), Laoshan Laboratory (No. LSKJ202202600), and Shandong Natural Science Foundation Project (ZR2019ZD12), Fundamental Research Funds for the Central Universities (201962009). Xin Qi is supported by the Young Scientists Fund of the National Natural Science Foundation of China (No. 42305019) and the Qingdao Postdoctoral Science Foundation (No. QDBSH20230102060). Yang Zhao is supported by the Taishan Scholar Foundation of Shandong Province (No. tsqn202408080). Zhaolu Hou is supported by Shandong Natural Science Foundation Project (ZR2020QD056). The NMME project and data dissemination is supported by NOAA, NSF, NASA and DOE.

Data availability All reanalysis and reforecast data in the study are publicly available. The ERA5 data can be accessed on https://cds-beta.climate.copernicus.eu/. The OISST dataset can be retrieved from https://www.ncei.noaa.gov/products/optimum-interpolation-sst. The GPCP dataset is available at https://climatedataguide.ucar.edu/climate-data/gpcp-monthly-global-precipitation-climatology-project. The NMME forecast data can be obtained from https://www.cpc.ncep.noaa.gov/products/NMME/.

Declarations

Conflict of interest The authors have no relevant financial or non-financial interests to disclose.

References

Becker E, Van den Dool, Zhang Q (2014) Predictability and Forecast Skill in NMME. J Clim 27:5891–5906. https://doi.org/10.1175/jcli-d-13-00597.1

Chen Y, Zhai P (2017) Simultaneous modulations of precipitation and temperature extremes in southern parts of China by the boreal summer intraseasonal oscillation. Clim Dyn 49:3363–3381. https://doi.org/10.1007/s00382-016-3518-4

Diallo I, Xue Y, Chen Q, Ren X, Guo W (2024) Effects of spring tibetan Plateau land temperature anomalies on early summer floods/droughts over the monsoon regions of South East Asia. Clim Dyn 62:2659–2681. https://doi.org/10.1007/s00382-021-06053-8

Gao M, Wang B, Yang J, Dong W (2018a) Are peak summer Sultry Heat Wave days over the Yangtze-Huaihe River Basin Predictable? J Clim 31:2185–2196. https://doi.org/10.1175/jcli-d-17-0342.1

Gao M, Yang J, Wang B, Zhou S, Gong D, Kim S-J (2018b) How are heat waves over Yangtze River valley associated with atmospheric quasi-biweekly oscillation? Clim Dyn 51:4421–4437. https://doi.org/10.1007/s00382-017-3526-z

Gao M, Yang J, Gong D, Shi P, Han Z, Kim S-J (2019) Footprints of Atlantic Multidecadal Oscillation in the low-frequency variation of Extreme High temperature in the Northern Hemisphere. J Clim 32:791–802. https://doi.org/10.1175/jcli-d-18-0446.1

Hersbach H, Bell B, Berrisford P et al (2020) The ERA5 global reanalysis. Q J R Meteorol Soc 146:1999–2049. https://doi.org/10.1002/qj.3803

Hsu P-C, Lee J-Y, Ha K-J, Tsou C-H (2017) Influences of Boreal Summer Intraseasonal Oscillation on Heat waves in Monsoon Asia. J Clim 3:7191–7211. https://doi.org/10.1175/jcli-d-16-0505.1

Hu K, Huang G, Huang R (2011) The impact of Tropical Indian Ocean variability on summer Surface Air Temperature in China. J Clim 24:5365–5377. https://doi.org/10.1175/2011jcli4152.1

Hua W, Dai A, Qin M, Hu Y, Cui Y (2023) How unexpected was the 2022 Summertime Heat extremes in the Middle reaches of the Yangtze River? Geophys Res Lett 50. https://doi.org/10.1029/2023gl104269

Huang B, Liu C, Banzon V, Freeman E, Graham G, Hankins B, Smith T, Zhang H-M (2021) Improvements of the Daily Optimum Interpolation Sea Surface temperature (DOISST) version 2.1. J Clim 34:2923–2939. https://doi.org/10.1175/jcli-d-20-0166.1

Kirtman BP, Min D, Infanti JM et al (2014) The north American Multimodel Ensemble Phase-1 Seasonal-to-interannual prediction; Phase-2 toward developing Intraseasonal Prediction. Bull Am Meteorol Soc 95:585–601. https://doi.org/10.1175/bams-d-12-00050.1

Leach NJ, Weisheimer A, Allen MR, Palmer T (2021) Forecast-based attribution of a winter heatwave within the limit of predictability. Proc Natl Acad Sci 118:9. https://doi.org/10.1073/pnas.2112087118

Li J-P, Zheng F, Sun C, Feng J, Wang J (2019) Pathways of influence of the Northern Hemisphere mid-high latitudes on east Asian climate: a review. Adv Atmos Sci 36:902–921. https://doi.org/10.1007/s00376-019-8236-5

Liu B, Zhu C, Ma S, Yan Y, Jiang N (2023) Subseasonal processes of triple extreme heatwaves over the Yangtze River Valley in 2022. Weather Clim 40. https://doi.org/10.1016/j.wace.2023.100572

Lu R, Chen R (2016) A review of recent studies on extreme heat in China. Atmos Ocean Sci Lett 9:114–121. https://doi.org/10.1080/16742834.2016.1133071

Luo M, Lau N-C (2017) Heat waves in Southern China: Synoptic Behavior, Long-Term Change, and Urbanization effects. J Clim 30:703–720. https://doi.org/10.1175/jcli-d-16-0269.1

Ma Y-Y, Chen Y-T, Hu X-X, Ma Q-R, Feng T-C, Feng G-L, Ma D (2023) The 2022 record-breaking high temperature in China: subseasonal stepwise enhanced characteristics, possible causes and its predictability. Adv Clim Change Res 14:651–659. https://doi.org/10.1016/j.accre.2023.09.008

Mariotti A, Ruti PM, Rixen M (2018) Progress in subseasonal to seasonal prediction through a joint weather and climate community effort. npj Clim Atmos Sci 1(4). https://doi.org/10.1038/s41612-018-0014-z

Patz JA, Campbell-Lendrum D, Holloway T, Foley JA (2005) Impact of regional climate change on human health. Nature 438:310–317. https://doi.org/10.1038/nature04188

Perkins SE (2015) A review on the scientific understanding of heatwaves-their measurement, driving mechanisms, and changes at the global scale. Atmos Res 164:242–267. https://doi.org/10.1016/j.atmosres.2015.05.014

Qi X, Yang J (2019) Extended-range prediction of a heat wave event over the Yangtze River Valley: role of intraseasonal signals. Atmos Ocean Sci Lett 12:451–457. https://doi.org/10.1080/16742834.2019.1669408

Qi X, Yang J, Gao M, Yang H, Liu H (2019) Roles of the Tropical/Extratropical Intraseasonal oscillations on Generating the Heat Wave over Yangtze River Valley: A Numerical Study. J Geophys Res-Atmos 124:3110–3123. https://doi.org/10.1029/2018jd029868

Quesada B, Vautard R, Yiou P, Hirschi M, Seneviratne SI (2012) Asymmetric European summer heat predictability from wet and dry southern winters and springs. Nature Clim Change 2:736–741. https://doi.org/10.1038/nclimate1536

Romanello M, Di Napoli C, Green C et al (2023) The 2023 report of the Lancet Countdown on health and climate change: the imperative for a health-centred response in a world facing irreversible harms. The Lancet 402:2346–2394. https://doi.org/10.1016/s0140-6736(23)01859-7

Schneider DP, Deser C, Fasullo J, Trenberth KE (2013) Climate data guide spurs discovery and understanding. Eos Trans AGU 94:121–122. https://doi.org/10.1002/2013eo130001

Sun Y, Li J (2022) Synergistic effect of El Nino and the North Pacific Oscillation on wintertime precipitation over Southeastern China and the East China Sea Kuroshio area. Clim Dyn 58:1635–1649. https://doi.org/10.1007/s00382-021-05982-8

Takaya K, Nakamura H (2001) A formulation of a phase-independent wave-activity flux for stationary and migratory quasigeostrophic eddies on a zonally varying basic flow. J Atmos Sci 58:608–627. https://doi.org/10.1175/1520-0469(2001)058%3C0608:Afoapi%3E2.0.Co;2

Tang X, Li J (2024) Synergistic effect of boreal autumn SST over the tropical and South Pacific and winter NAO on winter precipitation in the southern Europe. npj Clim Atmos Sci 7(1). https://doi.org/10.1038/s41612-024-00628-y

Tang S, Qiao S, Feng T, Fan P, Liu J, Zhao J, Feng G (2023a) Predictability of the unprecedented 2022 late summer Yangtze River Valley and Tibetan Plateau heatwaves by the NCEP CFSv2. Atmos Res 296. https://doi.org/10.1016/j.atmosres.2023.107053

Tang X, Li J, Zhang Y, Li Y, Zhao S (2023b) Synergistic effect of El Niño and negative phase of North Atlantic Oscillation on Winter Precipitation in the Southeastern United States. J Clim 3:1767–1791. https://doi.org/10.1175/jcli-d-22-0293.1

Teng H, Branstator G, Wang H, Meehl GA, Washington WM (2013) Probability of US heat waves affected by a subseasonal planetary wave pattern. Nat Geosci 6:1056–1061. https://doi.org/10.1038/ngeo1988

Vitart F, Ardilouze C, Bonet A et al (2017) The Subseasonal to Seasonal (S2S) Prediction Project Database. Bull Am Meteorol Soc 98:163–173. https://doi.org/10.1175/bams-d-16-0017.1

Wang P, Tang J, Sun X, Wang S, Wu J, Dong X, Fang J (2017) Heat waves in China: definitions, leading patterns, and connections to large-Scale Atmospheric circulation and SSTs. J Geophys Res-Atmos 122:10679–10699. https://doi.org/10.1002/2017jd027180

Wang H, Li J, Zheng F, Li F (2023a) The synergistic effect of the summer NAO and northwest pacific SST on extreme heat events in the central-eastern China. Clim Dyn 61:4283–4300. https://doi.org/10.1007/s00382-023-06807-6

Wang Z, Luo H, Yang S (2023b) Different mechanisms for the extremely hot central-eastern China in July-August 2022 from a eurasian large-scale circulation perspective. Environ Res Lett 18(2). https://doi.org/10.1088/1748-9326/acb3e5

Wei J, Ting D, Hui G, Lv Z (2024) China's Yangtze River basin is becoming the super heatwave centre in the east Asian monsoon regions. Int J Climatol 44:5028–5038. https://doi.org/10.1002/joc.8621

Wu ZW, Zhang P, Chen H, Li Y (2016) Can the Tibetan Plateau snow cover influence the interannual variations of Eurasian heat wave frequency? Clim Dyn 46:3405–3417. https://doi.org/10.1007/s00382-015-2775-y

Xie J, Yu J, Chen H, Hsu P-C (2020) Sources of Subseasonal Prediction Skill for heatwaves over the Yangtze River Basin revealed from three S2S models. Adv Atmos Sci 37:1435–1450. https://doi.org/10.1007/s00376-020-0144-1

Xu L, Chen N, Chen Z, Zhang C, Yu H (2021) Spatiotemporal forecasting in earth system science: methods, uncertainties, predictability and future directions. Earth Sci Rev 222. https://doi.org/10.1016/j.earscirev.2021.103828

Yang J, Zhu T, Gao M, Lin H, Wang B, Bao Q (2018) Late-July barrier for Subseasonal Forecast of Summer Daily Maximum Temperature over Yangtze River Basin. Geophys Res Lett 45:12610–12615. https://doi.org/10.1029/2018gl080963

Yang J, Zhu T, Vitart F, Wang B, Xiang B, Bao Q, Lee J-Y (2024) Synchronous eurasian heat extremes tied to boreal summer combined extratropical intraseasonal waves. npj Clim Atmos Sci 7(1). https://doi.org/10.1038/s41612-024-00714-1

Zhang L, Yu X, Zhou T, Zhang W, Hu S, Clark R (2023) Understanding and attribution of Extreme Heat and Drought events in 2022: current Situation and Future challenges. Adv Atmos Sci 40:1941–1951. https://doi.org/10.1007/s00376-023-3171-x

Zhao Q, Guo Y, Ye T et al (2021) Global, regional, and national burden of mortality associated with non-optimal ambient temperatures from 2000 to 2019: a three-stage modeling study. Lancet Planet Health 5:E415–E425

Zhou Y, Wu Z (2016) Possible impacts of Mega-el Nino/Southern Oscillation and Atlantic Multidecadal Oscillation on eurasian heatwave frequency variability. Q J R Meteorol Soc 142:1647–1661. https://doi.org/10.1002/qj.2759

Zhu Z, Li T (2018) Extended-range forecasting of Chinese summer surface air temperature and heat waves. Clim Dyn 50:2007–2021. https://doi.org/10.1007/s00382-017-3733-7

Zhu C, Wang B, Qian W, Zhang B (2012) Recent weakening of northern east Asian summer monsoon: a possible response to global warming. Geophys Res Lett 39. https://doi.org/10.1029/2012gl051155